Catalytic Activities of Transition Metal Phosphides for NO Dissociation and Reduction With CO

Z. Yao,[a,b,*] X. Qiao,[a] D. Liu,[a] Y. Shi,[a] and Y. Zhao[a]

[a]College of Chemistry, Chemical Engineering and Environmental Engineering, Liaoning Shihua University, Liaoning, PR China 113001

[b]Department of Chemistry, Dalian University of Technology, Dalian 116024, PR China

doi: 10.15255/CABEQ.2014.2133

Original scientific paper
Received: October 19, 2014
Accepted: November 26, 2015

A series of metal phosphides (MoP, WP, Co_2P, Fe_2P and Ni_2P) were synthesized by H_2-temperature-programmed reduction method. Amongst these phosphides, Fe_2P was found to show a considerably higher activity for NO dissociation than other phosphides. Herein, it was firstly used as a catalyst for NO reduction with CO. Although the Fe_2P catalyst showed an excellent activity for NO conversion to N_2, there was a competition between NO reduction by CO and Fe_2P oxidation by oxygen originated from NO dissociation. A complete equality of NO conversion and NO reduction degree can be obtained after increasing CO concentration in the system, which demonstrated that a catalytic redox cycle can be established on Fe_2P catalyst, and hence in-situ oxidation of bulk Fe_2P was avoided.

Key words:

Fe_2P, NO reduction, NO dissociation, catalytic redox cycle, bulk oxidation

Introduction

Transition metal phosphides are a group of compounds with interesting chemical/physical properties and potential applications in various fields, such as electronics, magnetism, photonics, catalysis, and so on[1–4]. In particular, metal phosphides (e.g. MoP, Ni_2P, WP, Fe_2P and Co_2P) have been used as catalysts and extensively studied for hydrotreating reactions[5–8]. Among these phosphides, MoP, Ni_2P and WP catalysts have shown significant promise in this regard because of their high activities and resistance to poisoning[9–10]. Therefore, they have been gradually explored as catalysts in many reactions, including N_2H_4 decomposition[11,12], carbon dioxide reforming of methane[13], hydrogen evolution reaction[2,14] and hydrogen oxidation reaction[15]. However, compared with phosphides of metals (Ni, Mo and W), Fe_2P has received far less attention due to its poor activity in hydrotreating reactions[6]. Recently, it has been found that a highly dispersed Fe_2P catalyst on activated carbon showed better performance and stability than an iron catalyst[16]. Yet its general catalytic properties have not been explored, and this remains an area of considerable challenge.

In this study, we firstly report that Fe_2P has a much higher catalytic activity for NO dissociation than phosphides of Ni, Mo, W and Co. In view of this unprecedented activity, Fe_2P was selected as the representative of phosphides to investigate the genuine nature of these catalysts for catalytic removal of NO. Although the activity and reaction mechanism of Fe_2P catalyst for NO reduction with H_2 had been studied in our previous letter[17], some important details were still missing about the development of a catalytic cycle in phosphide-catalyzed NO reduction reaction. Currently, the NO/CO reaction was used as a probe reaction to study the catalytic nature of Fe_2P catalyst. The route for keeping the catalyst stable and active was further perfected.

*Corresponding author: Zhiwei Yao, e-mail: mezhiwei@163.com, tel: +86-24-56860968

Experimental

Catalyst preparation

Phosphides of metals (Mo, W, Co, Fe and Ni) were prepared in two steps. In the first step, phosphate precursors were prepared by combining stoichiometric quantities of metal salt ($(NH_4)_6Mo_7O_{24}\cdot 4H_2O$, $(NH_4)_6H_2W_{12}O_{40}\cdot nH_2O$, $Co(NO_3)_2\cdot 6H_2O$, $Fe(NO_3)\cdot 9H_2O$ or $Ni(NO_3)_2\cdot 6H_2O$) and ammonium phosphate $(NH_4)_2HPO_4$ in sufficient distilled water to form a clear solution. In the case of Ni and Co, several drops of nitric acid were needed to give rise to homogeneous solution. Then the solution was evaporated to dryness and calcined in air at 500 °C for 5 h. In the second step of preparation, the phosphate precursors were converted into phosphides according to H_2-temperature-programmed reduction procedure described by Prins and co-workers[6]. Typical-

ly, about 2.0 g of phosphate precursor was placed in a micro-reactor and a flow of H_2 (150 cm^{-3} min^{-1}) was introduced into the system. The temperature was increased from room temperature (RT) to 650 °C at a rate of 1 °C min^{-1}, where it was held for 2 h before quenching to RT in a flow of H_2. Finally, the material was passivated in 1 % O_2/Ar for 12 h before it was exposed to air.

Catalyst characterization

XRD examination was performed using an X-ray diffractometer (Rigaku D-Max Rotaflex) with Cu *Kα* radiation (λ = 1.5404 Å) in the 2θ range from 20 to 90° at a step size of 0.06°. The sample particle size was estimated according to the Scherrer formula. The BET surface areas of passivated samples were measured on an ASAP 2010 instrument. The N_2 gas was used for standard five-point BET surface area measurements. A temperature-programmed surface reaction (TPSR) experiment was performed on a flow reaction system. The catalyst (0.4 g) was pretreated in He flow at 500 °C for 1 h, and then cooled to 150 °C. After thermal stability was reached, the temperature was raised to 500 °C at 15 °C min^{-1} in 1 % NO/1 % CO/He (50 cm^{-3} min^{-1}). The effluent gases were continuously monitored with a mass spectrometer (MS, HP G1800A) for the analysis of masses (M) = 30 (NO), M = 32 (O_2) and M = 28 (N_2 or CO), and an infrared absorption spectrometer (IRAS, SICK-MAIHAK-S710) for that of N_2O, CO and CO_2.

Catalyst activity

The catalytic activity was measured using a 6.0 mm (o.d.) silica reactor by feeding a gas mixture of 0.1 % NO/0–0.3 % CO/He. Typically, 0.4 g of catalyst was loaded onto a plug of silica wool, and the temperature of the catalyst bed was measured with a thermocouple inserted directly into the bed. The catalyst was pretreated in pure He at 400 °C for 1 h before the reaction. The reactants passed over the catalyst at a flow rate of 20 cm^3 min^{-1}, the corresponding W/F was 1.2 g s cm^{-3}. The effluent gases were monitored by online GC (HP 5890) using a molecular sieve 5A column (3 m, ϕ4) with a thermal conductivity detector (for the analysis of O_2, N_2, CO and NO), as well as a mass spectrometer (MS, HP G1800A) and an infrared absorption spectrometer (IRAS, SICK-MAIHAK-S710) (for that of CO_2, N_2O and other possible nitrogen oxides).

Results and discussion

XRD patterns of the as-prepared phosphides of metals (Mo, W, Co, Fe and Ni) are shown in Fig. 1.

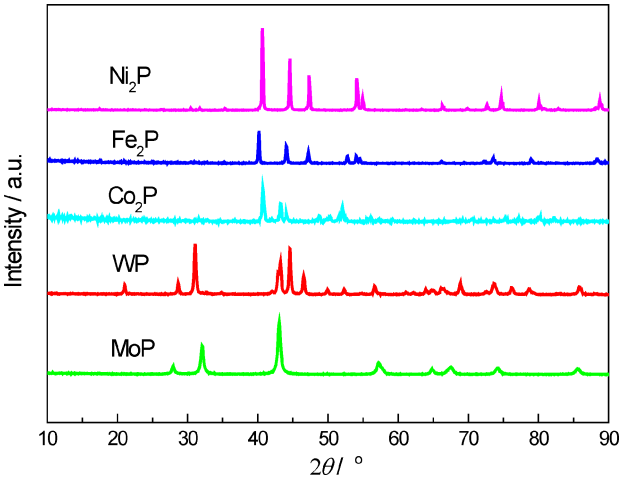

Fig. 1 – *XRD pattern of as-prepared MoP, WP, Co_2P, Fe_2P and Ni_2P catalysts*

Table 1 – *Characterization results of samples*

Sample	Crystalline phase	2q/°	BET area/ m^2 g^{-1}	Particle size/nm
MoP	MoP	28.1, 32.2, 43.2, 57.3	5.1	21
WP	WP	31.2, 43.3, 44.7, 46.7	5.7	32
Co_2P	Co_2P	40.9, 43.4, 44.2, 52.3	4.9	42
Fe_2P	Fe_2P	40.3, 44.2, 47.3, 52.9	3.6	36
Ni_2P	Ni_2P	40.8, 44.7, 47.4, 54.3	3.9	33

The peak positions were consistent with the crystalline phases listed in Table 1. There were no metal phosphates/oxides, and no signal of phosphide phases other than that of the observed one, indicating that the materials were phase-pure. Table 1 also summarizes the textural properties of these phosphides. All the phosphides obtained had lower surface area, from 3.6 to 5.7 m^2 g^{-1}. The crystal sizes were calculated by the Scherrer formula based on XRD peak broadening, indicating dimensions of the order 21–42 nm.

Subsequently, the catalytic activity of these materials was evaluated for NO dissociation, and the results are shown in Fig. 2. It can be observed that, over WP, MoP, Fe_2P, Co_2P and Ni_2P catalysts, the NO conversion to N_2 was about 0.003, 0.004, 0.037, 0.013 and 0.001 μmol g_{cat}^{-1} s^{-1} at 400 °C, respectively. Obviously, amongst this series of phosphides, Fe_2P was found to exhibit a considerably higher activity than other phosphide catalysts. However, it was worthy to note that the O_2 generated in NO decomposition was not detected in the reactions. Our previous study had proved that oxygen species produced during NO decomposition was not released into the gas phase as O_2 but captured by phosphide catalyst, which led to bulk oxidation of phosphide[17]. It was suggested that a catalytic redox

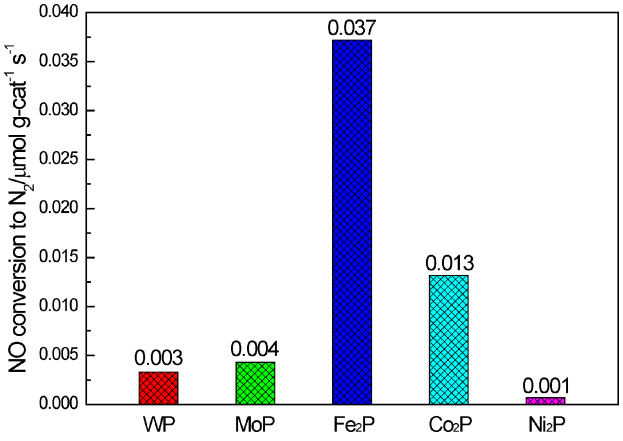

Fig. 2 – *NO conversion to N_2 at 400 °C over MoP, WP, Co_2P, Fe_2P and Ni_2P catalysts. Reaction conditions: NO = 1227 mg m^{-3}, W/F = 1.2 g s cm^{-3}, reaction time = 30 min.*

cycle could be established by introducing a reducing agent into the system so that the oxygen could be removed to avoid bulk oxidation of phosphide catalyst. Generally, redox reaction was dependent on reaction temperature and reaction gas composition. Therefore, the rest of this paper was devoted to investigate the temperature and composition dependence of NO/CO reaction over Fe_2P catalyst, and to give insights into the genuine nature of Fe_2P catalyst for catalytic removal of NO.

Table 2 lists the temperature dependence of NO and CO conversion in NO/CO (1:1 ratio) reaction over Fe_2P catalyst. It can be observed that the Fe_2P catalyst showed a high activity of ca. 100 % conversion of NO to N_2 in the temperature range 300–500 °C. Nevertheless, the conversion of CO was lower than that of NO at any temperature. The reaction we were expecting for the NO reduction with CO was stoichiometrically represented as:

$$2NO + 2CO \rightarrow N_2 + 2CO_2 \qquad (1)$$

Based on the results of TPO and O_2-uptake studies[17], the oxidation of Fe_2P occurred above 220 °C in an oxidation atmosphere. Therefore, it was deduced that the following oxidation of Fe_2P had occurred:

$$Fe_{lattice} + xO_{ad} \rightarrow FeO_x \qquad (2)$$

Table 2 – *Temperature dependence of NO and CO conversion in 1:1 NO:CO reaction over Fe_2P catalyst*

Temperature/°C	Reaction time/h	NO conversion to N_2/%	CO conversion/%
300	10	100	18
400	32	100	70
500	32	100	24

Reaction conditions: NO = 1227 mg m^{-3}, CO = 1145 mg m^{-3}, W/F = 1.2 g s cm^{-3}.

O_{ad} will be produced by NO dissociation.

$$NO_{ad} \rightarrow N_{ad} + O_{ad} \qquad (3)$$

Therefore, the conversion of NO to N_2 was higher than that of CO because of the production of N_2 during the reaction between oxygen (generated from NO dissociation) and Fe_2P catalyst. Obviously, there was a competition between NO reduction by CO (Eq. 1) and Fe_2P oxidation by oxygen species (Eqs. 2 and 3) in the system. The NO reduction with CO was an activated process, and a rise in temperature would enhance the reduction degree of NO. The CO conversion had a maximum (ca. 70 %) at 400 °C, indicating that NO reduction degree went through a maximum at this temperature. Above 400 °C, there was a sharp decrease in NO reduction probably due to the large extent of Fe_2P oxidation. It was hence suggested that the addition of CO concentration in NO/CO reaction at 400 °C was most likely to prevent bulk oxidation of Fe_2P catalyst.

Fig. 3 shows the effect of feed composition on the catalytic activity of Fe_2P catalyst in NO/CO reactions. It can be seen that the Fe_2P catalyst showed a stable activity (ca. 100 % conversion of NO to N_2) in a gas stream of 0.1 % NO/0.1 % CO/He at 400 °C, but deactivated quickly after 8 h of on-stream reaction: NO conversion to N_2 decreased from ca. 100% to ca. 65% within a period of 11 h. With the addition of CO in the feed, the Fe_2P catalyst showed a stable activity throughout the test period of 11 h, no matter whether it was in 0.1 % NO/0.2 % CO/He or 0.1 % NO/0.3 % CO/He. This result indicated that the lifetime of Fe_2P catalyst can be prolonged when the feed gas was rich in CO. To better analyze the effect of NO:CO compositions on the catalytic activity of Fe_2P catalyst, the NO and

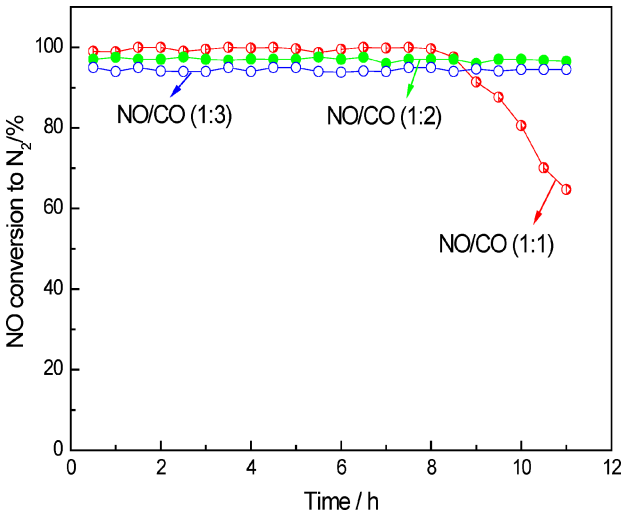

Fig. 3 – *Effect of feed composition on catalytic activity of Fe_2P catalyst in NO/CO reactions. Reaction conditions: NO = 1227 mg m^{-3}, CO = 1145–3436 mg m^{-3}, W/F = 1.2 g s cm^{-3}, reaction temperature = 400 °C.*

Table 3 – *Effect of feed composition on the catalytic activity of Fe_2P catalyst in NO/CO reactions*

CO:NO	NO conversion to N_2/%	CO conversion/%	NO reduction degree/%
1:1	100	62	62
2:1	97	41	82
3:1	96	32	96

Reaction conditions: NO = 1227 mg m^{-3}, CO = 1145–3436 mg m^{-3}, W/F= 0.15 g s cm^{-3}, reaction time = 8 h, reaction temperature = 400 °C.

CO conversion as well as NO reduction degree in NO/CO reactions at 400 °C are shown in Table 3. The nitrogen-containing gas products was only N_2, without N_2O and other nitrogen oxides by analysis of MS and IRAS. Thus, the NO reduction degree can be estimated by means of $([CO]_{in} - [CO]_{out})/[NO]_{in}$ ratio. As shown in Table 3, the conversion of NO to N_2 was closer in the three reactions. Additionally, reasonable trends can be observed that the consumption of CO increased when the feed composition became gradually richer in CO, and hence the NO reduction degree correspondingly increased. This was because an addition of CO in feed gas could increase the CO concentration on the Fe_2P surface, which helped in the reduction of NO by CO (Eq. 1), in contrast, suppressed Fe_2P oxidation by surface oxygen (Eqs. 2 and 3). Note that a complete equality of NO conversion and NO reduction degree appeared to be achieved when the NO:CO ratio decreased to 1:3. This result indicated that the CO concentration in feed gas with 1:3 NO:CO ratio was sufficient to remove surface oxygen and establish a catalytic cycle on Fe_2P catalyst.

In order to investigate the structural change of Fe_2P catalysts after reaction, the used Fe_2P catalysts (functioned in 0.1 % NO/0.1 % CO/He and 0.1 % NO/0.3 % CO/He, respectively, at 400 °C for 11 h) were characterized by XRD. As shown in Fig. 4, the Fe_2P catalyst used in 0.1 % NO/0.1 % CO/He for 11 h showed peaks of Fe_2O_3, Fe_3O_4 and FeP crystallites, and the signals of Fe_2P were untraceable. This was a clear indication that bulk Fe_2P can be oxidized completely by oxygen produced from NO dissociation in 0.1 % NO/0.1 % CO/He reaction. In other words, oxygen from NO dissociation would inevitably incorporate into the bulk of Fe_2P catalyst and hence could be removed completely by CO in the feed gas. Noticeably, the diffraction pattern for the Fe_2P catalyst used in 0.1 % NO/0.3 % CO/He for 11 h was identical to that of the fresh sample. These results indicated that a NO/CO ratio of 1/3 was required to avoid bulk oxidation of Fe_2P catalyst in NO/CO reaction, in good agreement with the results that a catalytic cycle can be established on

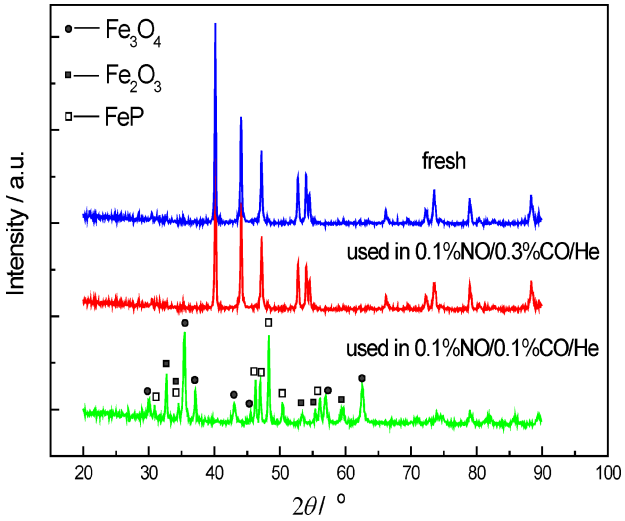

Fig. 4 – *XRD patterns of used Fe_2P samples as well as fresh sample for comparison*

Fe_2P catalyst in 0.1 % NO/0.3 % CO/He at 400 °C (Table 3).

In an attempt to understand the reaction mechanism of Fe_2P catalyst for NO reduction with CO, the TPSR experiment was performed to examine surface reactivity of NO and CO on Fe_2P catalyst. Fig. 5 shows the MS and IRAS profiles as a function of temperature during TPSR. It can be seen that the signals of M = 30 (NO) and M = 28 (N_2 or CO) began to decrease when the temperature was above ~220 °C. This result indicated that NO and CO species adsorption and dissociation, as well as the reaction between the two species had occurred, which was in agreement with the observation of IRAS profile that CO concentration decreased but CO_2 concentration increased above 220 °C, at the same time the production of N_2O peaks occurred at 270 °C. This was a clear indication that NO was mainly converted to N_2O between 220 and 270 °C. However, at temperatures above 270 °C, the concentration of N_2O decreased but that of M = 28 (N_2 or CO) increased, indicating that NO was mainly converted to N_2. Complete NO conversion plateau was obtained at about 300 °C, which was coincident with the signal of M = 28 (N_2 or CO) reaching a maximum. With the temperature increased to 400 °C, the signal of M = 28 (N_2 or CO) and the concentration of CO reached a lower value, but the CO_2 reached the maximum concentration. This demonstrated the highest degree of NO reduction by CO (Eq. 1) at this temperature. However, the change trend of the MS and IRAS profiles above 400 °C showed a decrease in the NO reduction degree. In other words, above 400 °C, the Fe_2P oxidation reaction (Eqs. 2 and 3) was becoming violent. These results agreed well with the data in Table 2.

Based on the TPSR and XRD results, the surface reactions of NO and CO over Fe_2P catalyst can be proposed as follows:

(1) NO dissociation and Fe_2P oxidation.

$$NO\ (g) + * \rightleftarrows NO\ * \quad (4)$$

$$NO\ * + * \rightleftarrows N\ * + O\ * \quad (5)$$

$$2N\ * \rightleftarrows N_2\ * + * \quad (6)$$

$$N_2\ * \rightleftarrows N_2\ (g) + * \quad (7)$$

$$NO\ (g) + NO\ * \rightleftarrows ON\ * NO \quad (8)$$

$$ON\ * NO + * \rightleftarrows N_2O\ * + O\ * \quad (9)$$

$$N\ * + NO\ * \rightleftarrows N_2O\ * + * \quad (10)$$

$$N_2O\ * \rightleftarrows N_2O\ (g) + * \quad (11)$$

$$xO\ * + Fe_2P \rightarrow FeO_x + FeP \quad (12)$$

In view of the fact that there was no O_2 species detected in NO/CO reaction (see Fig. 5a), it was reasonable to deduce that the oxygen produced during NO dissociation was partly released into the gas phase as N_2O (g); the rest was captured by Fe_2P catalyst. Heavy accumulation of surface oxygen resulted in gradual diffusion of oxygen into the Fe_2P lattice, and would cause the ultimate oxidation of the bulk.

(2) NO reduction with CO.

After introducing CO into the system at an appropriate reaction temperature, the poisonous effect of oxygen toward Fe_2P can be eliminated by regulating the CO concentration in the feed; the process can be described as follows:

$$CO\ (g) + * \rightleftarrows CO* \quad (13)$$

$$CO* + O* \rightleftarrows CO_2* \quad (14)$$

$$CO_2* \rightleftarrows CO_2\ (g) + * \quad (15)$$

According to the results of activity studies and XRD characterization (Table 3 and Fig. 4), a minimum of 0.3 % of CO in the 0.1 % NO/He feed was required for establishing a catalytic cycle and avoiding bulk oxidation of Fe_2P catalyst.

ACKNOWLEDGMENTS

The work was supported by the National Natural Science Foundation of China (No. 21276253 and No. 21006032).

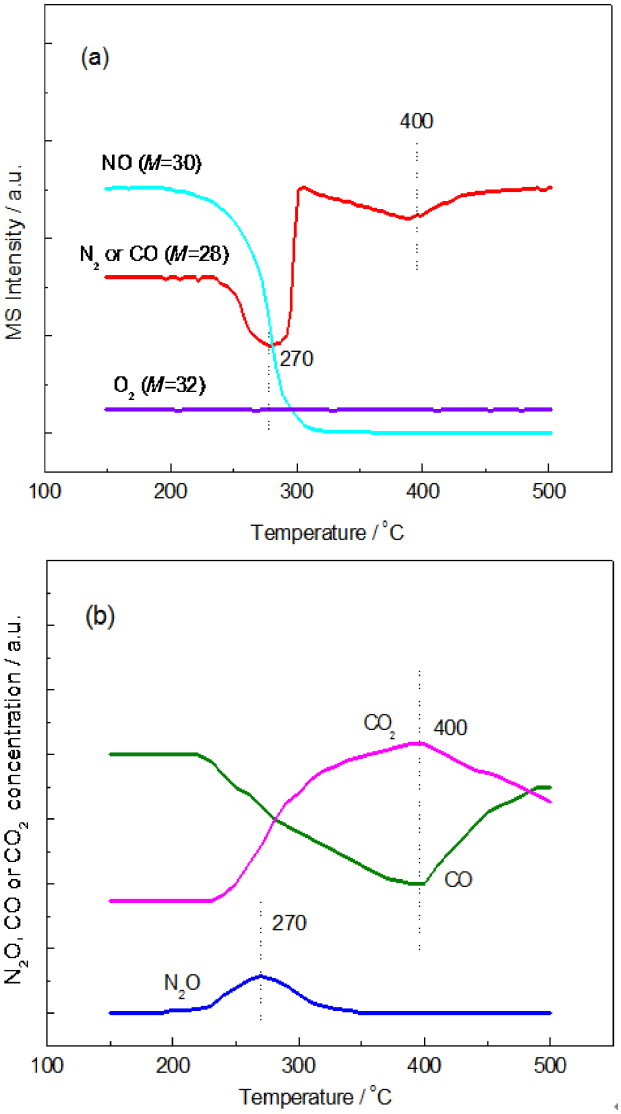

Fig. 5 – *TPSR of Fe_2P catalyst followed by (a) MS and (b) IRAS*

List of symbols

W – weight of catalyst, g

F – flow rate of feeding gas, $cm^3\ min^{-1}$

References

1. *Yoon, K. Y., Jang, Y., Park, J., Hwang, Y., Koo, B., Park, J.-G., Hyeon, T.*, Synthesis of uniform-sized bimetallic iron–nickel phosphide nanorods, J. Solid State Chem. **181** (2008) 1609. doi: http://dx.doi.org/10.1016/j.jssc.2008.05.022
2. *Popczun, E. J., McKone, J. R., Read, C. G., Biacchi, A. J., Wiltrout, A. M., Lewis, N. S., Schaak, R. E.*, Nano structured Nickel Phosphide as an Electro catalyst for the Hydrogen Evolution Reaction, J. Am. Chem. Soc. **135** (2013) 9267. doi: http://dx.doi.org/10.1021/ja403440e
3. *Jiang, X. C., Xiong, Q. H., Nam, S., Qian, F., Li, Y., Lieber, C. M.*, InAs/InP Radial Nanowire Heterostructures as High Electron Mobility Devices, Nano Lett. **7** (2007) 3214. doi: http://dx.doi.org/10.1021/nl072024a

4. *Alexander, A.-M., Hargreaves, J. S. J.,* Alternative catalytic materials: carbides, nitrides, phosphides and amorphous boron alloys, Chem. Soc. Rev. **39** (2010) 4388. doi: http://dx.doi.org/10.1039/B916787K
5. *Brock, S. L., Senevirathne, K.,* Recent developments in synthetic approaches to transition metal phosphide nanoparticles for magnetic and catalytic applications, J. Solid State Chem. **181** (2008) 1552. doi: http://dx.doi.org/10.1016/j.jssc.2008.03.012
6. *Oyama, S. T.,* Novel catalysts for advanced hydroprocessing: Transition metal phosphides, J. Catal. **216** (2003) 343. doi: http://dx.doi.org/10.1016/S0021-9517(02)00069-6
7. *Oyama, S. T., Gott, T., Zhao, H., Lee, Y.-K.,* Transition metal phosphide hydroprocessing catalysts: A review, Catal. Today **143** (2009) 94. doi: http://dx.doi.org/10.1016/j.cattod.2008.09.019
8. *Shu, Y., Oyama, S. T.,* Synthesis, characterization, and hydro treating activity of carbon-supported transition metal phosphides, Carbon **43** (2005) 1517. doi: http://dx.doi.org/10.1016/j.carbon.2005.01.036
9. *Wang, A., Ruan, L., Teng, Y., Li, X., Lu, M., Ren, J., Wang, Y., Hu, Y.,* Hydrodesulfurization of dibenzothiophene over siliceous MCM-41-supported nickel phosphide catalysts, J. Catal. **229** (2005) 314. doi: http://dx.doi.org/10.1016/j.jcat.2004.09.022
10. *Clark, P. A., Oyama, S. T.,* Alumina-supported molybdenum phosphide hydro processing catalysts, J. Catal. **218** (2003) 78. doi: http://dx.doi.org/10.1016/S0021-9517(03)00086-1
11. *Cheng, R., Shu, Y., Zheng, M., Li, L., Sun, J., Wang, X., Zhang, T.,* Molybdenum phosphide, a new hydrazine decomposition catalyst: Micro calorimetry and FTIR studies, J. Catal. **249** (2007) 397. doi: http://dx.doi.org/10.1016/j.jcat.2007.04.007
12. *Ding, L., Shu, Y., Wang, A., Zheng, M., Li, L., Wang, X., Zhang, T.,* Preparation and catalytic performances of ternary phosphides NiCoP for hydrazine decomposition, Appl. Catal. A **385** (2010) 232. doi: http://dx.doi.org/10.1016/j.apcata.2010.07.020
13. *Yang, C., Li, X., Yang, Y., Yang, X., Yang, A.,* Study on a New Catalyst Tungsten Phosphide for the Carbon Dioxide Reforming of Methane and Its Preparation Conditions, Asian J. Chem. **25** (2013) 3601. doi: http://dx.doi.org/10.14233/ajchem.2013.13675
14. *Xiao, P., Sk, M. A., Thia, L., Ge, X., Lim, R. J., Wang, J.-Y., Lim, K. H., Wang, X.,* Molybdenum phosphide as an efficient electro catalyst for the hydrogen evolution reaction, Energy Environ. Sci. **7** (2014) 2624. doi: http://dx.doi.org/10.1039/C4EE00957F
15. *Izhar, S., Nagai, M.,* Transition metal phosphide catalysts for hydrogen oxidation reaction, Catal. Today **146** (2009) 172. doi: http://dx.doi.org/10.1016/j.cattod.2009.01.036
16. *Donald, J., Xu, C., Hashimoto, H., Byambajav, E., Ohtsuka, Y.,* Novel carbon-based Ni/Fe catalysts derived from peat for hot gas ammonia decomposition in an inert helium atmosphere, Appl. Catal. A **375** (2010) 124. doi: http://dx.doi.org/10.1016/j.apcata.2009.12.030
17. *Yao, Z. W., Dong, H., Shang, Y.,* Catalytic activities of iron phosphide for NO dissociation and reduction with hydrogen, J. Alloys. Compd. **474** (2009) L10. doi: http://dx.doi.org/10.1016/j.jallcom.2008.06.072